Analytical Letters

ISSN: 0003-2719 (Print) 1532-236X (Online) Journal homepage: https://www.tandfonline.com/loi/lanl20

Electrochemical Determination of Tyrosine using a Novel Tyrosinase Multi-Walled Carbon Nanotube (MWCNT) Polysulfone Modified Glassy Carbon Electrode (GCE)

Lisebo Phelane, Carla Gouveia-Caridade, Madalina M. Barsan, Priscilla G. L. Baker, Christopher M. A. Brett & Emmanuel I. Iwuoha

To cite this article: Lisebo Phelane, Carla Gouveia-Caridade, Madalina M. Barsan, Priscilla G. L. Baker, Christopher M. A. Brett & Emmanuel I. Iwuoha (2019): Electrochemical Determination of Tyrosine using a Novel Tyrosinase Multi-Walled Carbon Nanotube (MWCNT) Polysulfone Modified Glassy Carbon Electrode (GCE), Analytical Letters, DOI: 10.1080/00032719.2019.1649417

To link to this article: https://doi.org/10.1080/00032719.2019.1649417

Published online: 06 Aug 2019.

ANALYTICAL LETTERS
https://doi.org/10.1080/00032719.2019.1649417

Taylor & Francis
Taylor & Francis Group

ELECTROCHEMISTRY

Electrochemical Determination of Tyrosine using a Novel Tyrosinase Multi-Walled Carbon Nanotube (MWCNT) Polysulfone Modified Glassy Carbon Electrode (GCE)

Lisebo Phelane[a,b], Carla Gouveia-Caridade[b], Madalina M. Barsan[b], Priscilla G. L. Baker[a], Christopher M. A. Brett[b], and Emmanuel I. Iwuoha[a]

[a]Department of Chemistry, University of the Western Cape, Bellville, South Africa; [b]Department of Chemistry, Faculty of Sciences and Technology, University of Coimbra, Coimbra, Portugal

ABSTRACT

The modification of polysulfone (PSF) with multi-walled carbon nanotubes (MWCNT) is presented as a platform for the development of a tyrosinase biosensor. PSF, dissolved in dichloromethane, was deposited on a glassy carbon electrode (GCE), after which MWCNT functionalized in nitric acid, was drop coated on the PSF layer. Tyrosinase enzyme (TyOx), crosslinked with glutaraldehyde, was subsequently deposited on the MWCNT/PSF/GCE transducer to constitute the tyrosinase biosensor. The MWCNT/PSF/GCE (sensor) and TyOx/MWCNT/PSF/GCE (biosensor) were characterized using cyclic voltammetry and electrochemical impedance spectroscopy. Scanning electron microscopy was used to study the morphological changes after each modification step. Cyclic voltammetry measurements confirmed that MWCNT/PSF/GCE was a better platform for the direct detection of tyrosine than MWCNT/GCE or PSF/GCE. A well-defined analytical peak at 0.79 V with respect to Ag/AgCl was observed that was clearly distinguishable from the background current. The tyrosinase biosensor showed a very low limit of detection (0.3 nM) and a very high sensitivity (1.988 μA $\mu M^{-1} cm^{-2}$) towards tyrosine detection compared to comparable devices reported in the literature.

ARTICLE HISTORY
Received 5 June 2019
Accepted 24 July 2019

KEYWORDS
Biosensor; L-tyrosine; multi-walled carbon nanotube; polysulfone; tyrosinase

Introduction

Melanoma is a type of skin cancer which is formed from pigment-containing cells in the skin called melanocytes (Ly, Yoo, and Lee 2012). Melanocytes produce the dark pigment called melanin. Melanin is a pigment derived from the amino acid tyrosine responsible for the skin and hair color in living organisms and plays an important role in protecting the skin against ultraviolet light induced damage (Ly, Yoo, and Lee 2012; Lupu et al. 2013; Revin and John 2013).

Tyrosinase mRNA is an important biomarker for melanoma and a key factor in melanogenesis. Tyrosinase catalyzes the rate-limiting step in melanogensis via hydroxylation of tyrosine to 3,4-dihydroxy-L-phenylalanine (L-DOPA) and subsequent oxidation to

CONTACT Priscilla Baker pbaker@uwc.ac.za Department of Chemistry, University of the Western Cape, Private Bag X17, Bellville 7535, South Africa.
Color versions of one or more of the figures in the article can be found online at www.tandfonline.com/lanl.

dopaquinone (Revin and John 2013). During melanin biosynthesis, L-tyrosine is the starting material converted to L-DOPA and the ratio of these two compounds is an important indicator for the development of melanoma (Lupu et al. 2013; Revin and John 2013).

Tyrosinase is an enzyme made up of two histidine-coordinated copper atoms. The copper atoms are coordinated to the protein by six histidine residues in a paired helical bundle (Lupu et al. 2013). In the presence of oxygen, tyrosinase catalyzes two different enzymatic reactions: firstly the ortho-hydroxylation of monophenols to o-diphenols and secondly the oxidation of o-diphenols to o-quinones (Akyilmaz, Yorganci, and Asav 2010; Litescu, Eremia, and Radu 2010). Tyrosinase has been used widely in biosensor assembly for the determination of phenolic compounds.

Wang et al. (2008) developed a biosensor for the detection of catechol using a glassy carbon electrode (GCE) modified with tyrosinase-Fe_3O_4 magnetic nanoparticles-chitosan nanobiocomposite film (S. Wang et al. 2008). In another study (Y. Wang et al. 2010), a Fe_3O_4-chitosan nanocomposite was employed for the amperometric detection of dopamine through the biocatalytically liberated dopaquinone at -0.25 V with respect to saturated calomel electrode (Sanz et al. 2005; Wang et al. 2010; Karim and Jin 2013). Sanz et al. (2005), designed a tyrosinase biosensor based on the immobilization of the enzyme on a GCE modified with electrodeposited gold nanoparticles for determining phenolic compounds. The biosensor exhibited a rapid response to the changes in the substrate concentration for all of the phenolic compounds characterized that included phenol, catechol, caffeic acid, chlorogenic acid, and gallic acid (Sanz et al. 2005).

Carbon nanotubes (CNT) have attracted huge interest in various applications of engineering and technology due to their unique chemical, mechanical and electronic properties. The high conductivity, electrocatalytic and electrochemical properties of CNT have made them very attractive components of electrochemical sensors and biosensors (Samuel, Pumera, and Esteve 2007; Karim and Jin 2013). However, there are two major factors limiting the effectiveness of CNT.

Firstly, the dispersion of nanotubes is not always uniform. Due to their chemical structure and surface area, individual CNT form strong Van der Waals bonds with neighboring CNTs, which result in agglomeration of CNTs in various matrices. Secondly, interfacial bonding between CNT and polymer molecules due to the inert nature of the nanotubes prevent their uniform dispersion (Kim et al. 2002; Samuel, Pumera, and Esteve 2007).

The modification of the surface of carbon nanotubes by covalent or non-covalent functionalization is a possible solution for these problems (Karim and Jin 2013). Non-covalent surface modification is relatively common, where polymer chains are wrapped around the nanotubes or different surfactant molecules are adsorbed or physically bound to the CNT surface (Connell et al. 2001). Non-covalent functionalization of nanotubes based on colloid stabilization principles has been reported (Connell et al. 2001; Ke et al. 2007; Carvalho, Gouveia-Caridade, and Brett 2010).

For example, purified single-walled carbon nanotubes were mixed with charged ZrO_2 nanoparticle aqueous solutions and sonicated (Connell et al. 2001). The suspensions were allowed to stand for a few days to remove unstable large bundles of nanotubes. The remaining suspension of nanotubes with nanoparticles was observed to be transparent and very stable for long periods of time.

In covalent surface modification, polymer chains can be grafted on the surface of the nanotubes. Covalent functionalization of CNT is essential when the load transfer properties are important. Chemical functionalization of nanotubes offers the advantage of strengthening the composite by filling defects in the wall structure.

Chitosan, a low molecular weight green polymer, was covalently bound to the sidewalls of multi-walled carbon nanotubes (MWCNT) through nucleophilic substitution reaction (Ke et al. 2007; Carvalho, Gouveia-Caridade, and Brett 2010; Kaushik et al. 2012; Dyachkova et al. 2013). The amino acid and primary hydroxyl groups of chitosan were identified to be the main contributors to the formation of MWCNT–chitosan structures. These groups react with COCl groups generated on the CNT surfaces by acid treatment (Koziol, Boskovic, and Yahya 2010; Kaushik et al. 2012; Dyachkova et al. 2013).

Polysulfone (PSF) is a polymer with poor conductivity, but is widely used in membrane technology due to its solubility properties and its high thermal, chemical and mechanical resistance. The modification of these polymers is a challenge in polymer and membrane technologies. PSF is widely used in the manufacture of medical devices, membrane filtration systems, gas separation membranes and in energy storage devices (Park et al. 2006; Muya et al. 2014; Phelane et al. 2014).

Qiu et al. (2009) reported on blends of PSF and functionalized MWCNT dissolved in dimethylformamide which were used to prepare ultrafiltration membranes by a classical phase-inversion method (Qiu et al. 2009). The results showed that the quantity of functionalized MWCNTs was an important factor influencing the morphology and permeation properties of the blended membranes (Koziol, Boskovic, and Yahya 2010; Kaushik et al. 2012; Dyachkova et al. 2013). Park and coworkers, synthesized amphiphilic graft copolymers having PSF backbones and poly(ethylene glycol) (PEG) side chains (Park et al. 2006). The resulting PSF-graft-poly(ethylene glycol) (PSF-g-PEG) materials were hydrophilic but water insoluble. These properties make them suitable candidates for biomaterial coatings, such as for PSF-g-PEG modified membranes (Park et al. 2006; Qiu et al. 2009; Koziol, Boskovic, and Yahya 2010; Kaushik et al. 2012).

Here is reported the modification of PSF with MWCNTs for the design of a novel tyrosinase biosensor and its application to the quantitative detection of tyrosine in aqueous systems. The transducer was composed of PSF polymer modified with MWCNTs drop-coated on a GCE. The PSF casting suspension was prepared by dissolving PSF in dichloromethane. Bamboo-shaped MWCNTs were functionalized using HNO_3. The sensor systems were characterized using cyclic voltammetry (CV) and electrochemical impedance spectroscopy (EIS). Scanning electron microscopy (SEM) was used to study the morphology changes as a function of the layer by layer modification of the GCE surface.

Experimental

Chemicals and reagents

All chemicals were of analytical reagent grade and used as received without any further purification. Tyrosinase (from mushrooms), tyrosine, glutaraldehyde (GA) and PSF beads were purchased from Sigma-Aldrich. Multiwalled carbon nanotubes were purchased from NanoLab, USA, with 95% purity, 30 ± 10 nm diameter and 1–5 μm length.

Instrumentation and methods

Preliminary voltammetric studies were carried out using an Ivium CompactStat potentiostat (Ivium Technologies, Utrecht, Netherlands). Further measurements were carried out using a PalmSens potentiostat from Palm Instruments BV, Netherlands, operated using PS 4.4 software.

Electrochemical impedance spectroscopy (EIS) was performed using a Solartron 1250 Frequency Response Analyzer coupled to a Solartron 1286 Electrochemical Interface (Solartron Analytical, UK) controlled by Zplot software. A sinusoidal voltage perturbation of amplitude 10 mV rms was applied at frequencies ranging from 65 kHz to 10 mHz with 10 frequency steps per decade. The impedance data was modeled as simple Randles equivalent electrical circuits using ZView Software (Scribner Associates, USA). Some EIS measurements were carried out using IM6ex ZAHNER Elektrik instrument driven by Thales Software. However the experimental parameters of amplitude, frequency range and frequency response was kept the same for all impedance experiments.

A three-electrode system was used for all electrochemical experiments. The working electrode was an unmodified or modified GCE (area 0.071 cm^2) with a platinum wire as the counter electrode and Ag/AgCl (3M NaCl) as reference electrode.

Scanning electron microscopy (SEM) measurements were carried out using a LEO 1450 instrument. Enhanced images were obtained using a Zeiss Auriga (FEGSEM) field emission gun scanning electron microscope. Samples were coated with conductive carbon to enhance charge dissipation and improve imaging of the prepared materials.

Preparation of PSF

The preparation of a 0.05 g mL^{-1} PSF suspension was achieved by dissolving 0.5 g of PSF in 10 mL dichloromethane at room temperature and sonicating until a clear homogenous casting suspension was obtained.

Functionalization of MWCNT

The functionalization was done similarly to previous reports (Carvalho, Gouveia-Caridade, and Brett 2010; Peça, Bertotti, and Brett 2011). A mass of 0.1 g MWCNT was stirred into 10 mL of 3 M nitric acid (HNO_3) solution overnight. The solid product was filtered and washed with distilled water several times until the filtrate solution was neutral (pH 7). The resultant MWCNT were dried in an oven at 70 °C for 24 h.

From these functionalized MWCNTs, a 1% suspension of MWCNT was prepared by dispersing an appropriate mass of MWCNT in dimethylformamide.

Preparation of PSF/MWCNTs composite

10 µL of the PSF suspension was drop coated on a GC working electrode followed by two additions of 10 µL of MWCNT solution to produce a MWCNT/PSF/GCE sensor for electrochemical evaluation.

Fabrication of the TyOx/MWCNT/PSF/GCE

The tyrosinase biosensor was prepared by drop coating tyrosinase on the prepared MWCNT/PSF/GCE sensor platform and crosslinking with GA (Scheme 1).

Results and discussion

Scanning electron microscopy characterization

SEM was used to evaluate changes in the morphology of the electrode interface after each modification step (Figure 1).

The SEM image of PSF showed uniform morphology and well-defined hemispherical shaped pores, with pore size from 1 to 6 µm (Figure 1a). The MWCNTs, displayed in Figure 1b, showed the expected fibrous morphology of nanotubes with evidence of clustering and agglomeration. CNTs are held together by strong Van der Waals bonds between neighboring CNT, resulting in the formation of large aggregates (Dyachkova et al. 2013; Bidsorkhi et al., 2016).

The MWCNT/PSF composite layer (Figure 1c), showed spheres of different sizes, which were interpreted as the combined morphology features of the individual components. The pores observed in the SEM image of PSF alone disappeared after modification with CNTs due to a filler effect of the CNTs inserted into the polysulphone matrix. Additionally, the MWCNTs showed a very even distribution within the polymer due to the lyophilic properties of the CNTs. The carboxylic groups of the CNTs increase their

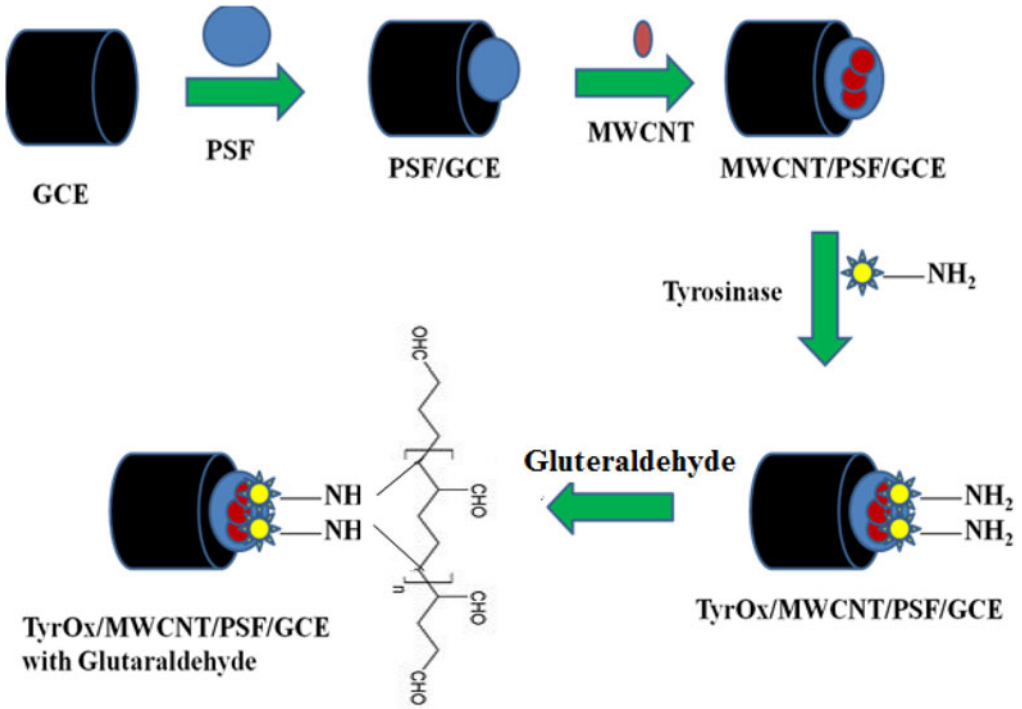

Scheme 1. Schematic diagram of the tyrosinase biosensor preparation.

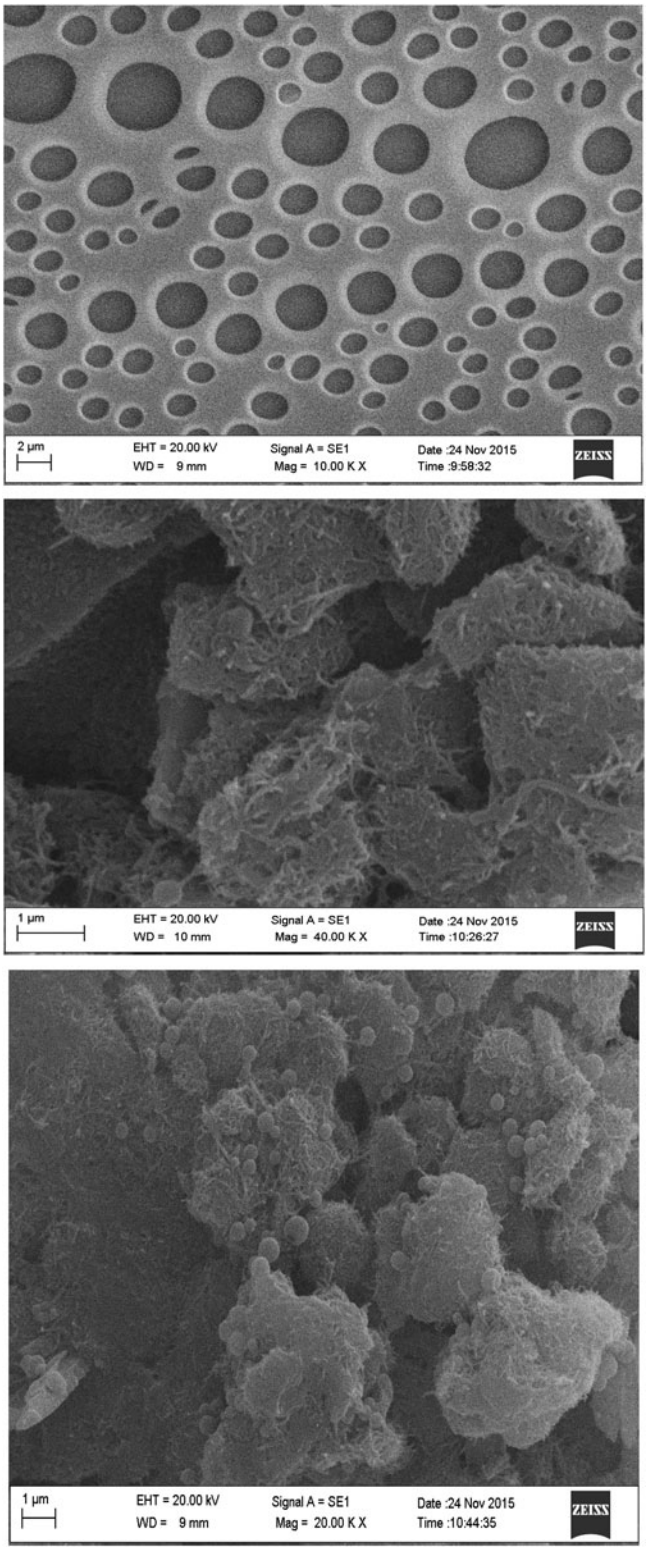

Figure 1. Morphological images for the: (a) polysulfone, (b) multi-walled carbon nanotubes and (c) MWCNT/PSF composite on a high resolution scanning electron microscope at 20 kV.

interactions with the polar solvent and possibly with dissolved PSF (Singjai, Changsarn, and Thongtem 2007; Bidsorkhi et al., 2016).

Cyclic voltammetric characterization of the prepared composite material

Cyclic voltammetry was used to characterize the GCE electrode modified with PSF and MWCNTs, as well as the layer-by-layer deposited MWCNT/PSF/GCE electrode. All electrochemistry experiments were performed in 10 mL of 0.1 M phosphate buffer (PBS at pH 7.0) at scan rates ranging from 10 to 200 mV s^{-1} in the potential range from 0 to 1000 mV with respect to Ag/AgCl. The oxidation of L-tyrosinase was recorded following the addition of 10 μL aliquots of 0.1 M L-tyrosine to the electrochemical cell.

The cyclic voltammograms obtained at the three electrodes (Figure 2) clearly highlight the contribution of MWCNTs in facilitating the oxidation of L-tyrosine. The peak potential for L-tyrosine oxidation at PSF/GCE was observed at 0.79 V with respect to Ag/AgCl, whereas MWCNT/GCE and MWCNT/PSF/GCE provided oxidation potentials of 0.70 and 0.67 V, respectively. The L-tyrosine peak observed at the MWCNT modified electrodes also showed better resolution of the oxidation peak and the highest oxidation currents of the three evaluated electrodes.

The oxidation of L-tyrosine was observed as a single peak with no evidence of a coupled reduction peak, indicating that the redox behavior of L-tyrosine is irreversible. The cyclic voltammetry of MWCNT/PSF/GCE showed that incorporating the MWCNTs into the PSF matrix results in a well-defined peak for L-tyrosine at 0.67 V. This peak was used as the analytical peak for reporting the oxidation of L-tyrosine.

The approximate surface concentrations of the three modified electrodes were determined from the plot of peak current with respect to scan rate using the Brown Anson model:

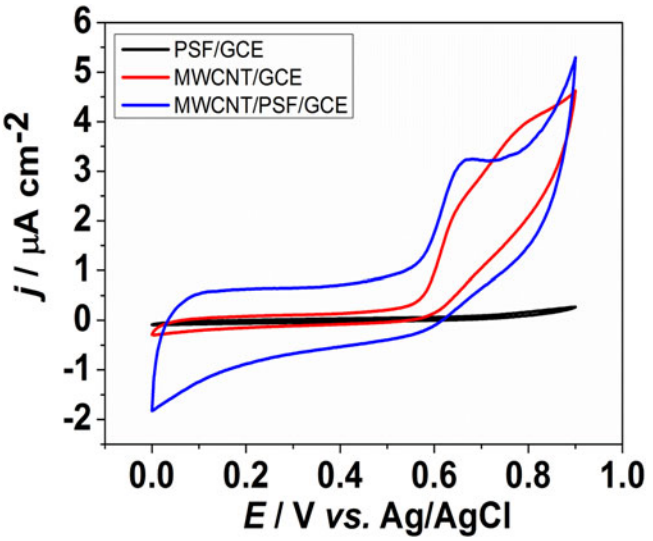

Figure 2. Cyclic voltammograms of 0.1 M L-tyrosine oxidation in 0.1 M phosphate buffer at pH 7.0 measured at the (black) PSF/GCE, (red) MWCNT/GCE and (blue) MWCNT/PSF/GCE at 50 mV s^{-1}.

Table 1. Surface concentrations of PSF/GCE, MWCNT/GCE and MWCNT/PSF/GCE determined by Brown Anson treatment of the CV measurements.

Electrode Material	Slope ($\mu A\ cm^{-2}/Vs^{-1}$)	R-squared	Surface concentration (mol cm^{-2})
PSF/GCE	1.405	0.999	5.26×10^{-12}
MWCNT/GCE	34.318	0.998	1.28×10^{-10}
MWCNT/PSF/GCE	37.597	0.998	1.41×10^{-10}

$$Ip = \frac{n^2\ F^2\ \Gamma^* A\ v}{4\ RT} \quad (1)$$

where n is the number of electrons transferred, F is the Faraday constant (96584 C mol^{-1}), Γ^* is the surface concentration (mol cm^{-2}), ν is the scan rate (V s^{-1}), R is gas constant (8.314 J mol^{-1} K^{-1}), and T is absolute temperature (298 K). A, the geometric surface area of the electrode (0.071 cm^2), was used in all calculations. Using this approach, a relative appreciation of the effect of surface modification was developed.

The surface concentration of the electroactive material increased significantly as a result of the incorporation of MWCNT (Table 1). In a Randles Sevçik treatment of the same measurements, a plot of peak current versus the square root of scan rate was observed as a linear plot over the range 10–200 mV s^{-1}, indicating that the oxidation of L-tyrosine at the MWCNT/GCE and MWCNT/PSF/GCE modified electrodes obeyed diffusion-controlled behavior (Xu and Wang 2005; Ma et al. 2010; Fauziyah et al. 2012; Wei et al. 2012).

Electrochemical impedance characterization of PSF/GCE, MWCNT/GCE and MWCNT/PSF/GCE

Electrochemical impedance spectroscopy is a frequency-dependent technique used to separate charge transfer processes from capacitive processes through equivalent circuit modeling. Experiments were performed with each modified electrode as the working electrode fixed at a potential of 0.7 V with respect to Ag/AgCl in 0.1 M PBS (Figure 3).

The equivalent circuit used to fit the EIS data was composed of the solution resistance (R_s), in series with a constant phase element (*CPE*) representing the interfacial charged double layer in parallel with the charge transfer resistance (R_{ct}). An open Warburg element (W_o) was introduced to model the diffusion of analyte across the concentration gradient in the cell (Figure 4; Xu and Wang 2005). The charge transfer resistance obtained from equivalent circuit fitting confirmed a dramatic decrease in magnitude as a direct result of MWCNT incorporation (Figure 5) into the MWCNT/PSF/GCE and MWCNT/GCE, yielding values of 3.78 and 5.40 kΩ, respectively.

The cyclic voltammetry of L-tyrosine showed that MWCNT/PSF/GCE gives the highest current observed from the impedance spectra, which was found to be in good agreement with the low R_{ct} for tyrosine oxidation.

Quantitative determination of L-tyrosine at MWCNT/PSF/GCE and TyrOx/MWCNT/PSF/GCE

For the determination of L-tyrosine at the sensor and biosensor platforms, CV was used to measure the change in current after each addition of L-tyrosine by scanning from 0

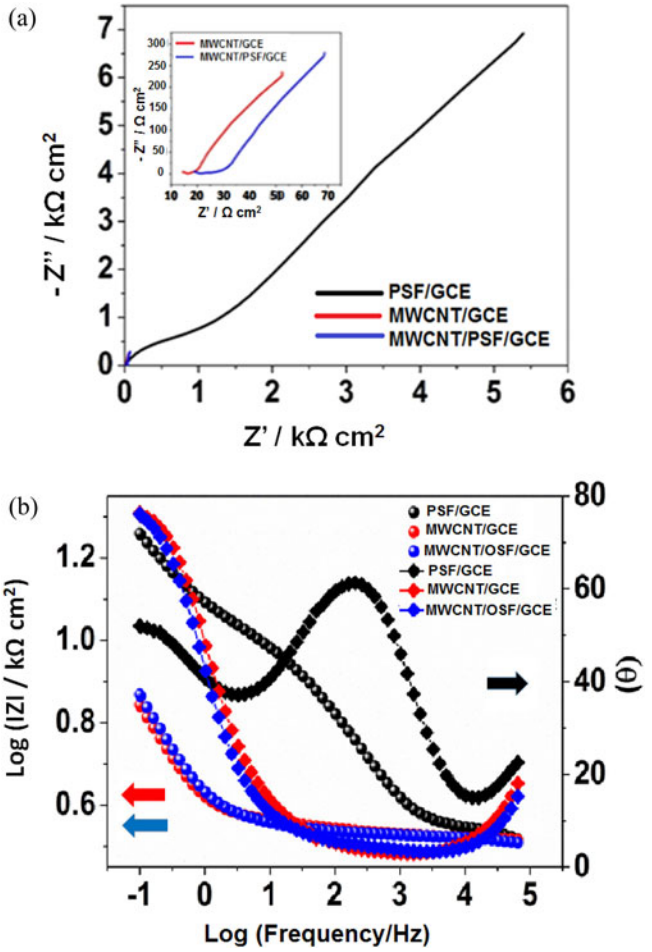

Figure 3. (a) Nyquist and (b) Bode plots for the PSF/GCE, MWCNT/GCE and MWCNT/PSF/GCE electrodes in 0.1 M phosphate buffer at pH 7.0 using a fixed potential of 0.7 V with respect to Ag/AgCl. The inset is enlargement of the high frequency region of the Nyquist plot.

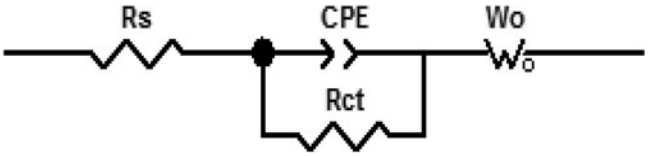

Figure 4. Equivalent circuit used to fit all of the impedance measurements comprised of the solution resistance (R_s), charge transfer resistance (R_{ct}), constant phase element (CPE) and Warburg element (W_o).

to 0.9 V at a scan rate of 50 mV s^{-1}. Consecutive additions of L-tyrosine gave final concentrations in the cell in the range from 1.96×10^{-6} to 3.94×10^{-4} M.

An irreversible anodic peak at 0.7 V was observed for the oxidation of L-tyrosine (Figures 6 and 7) and was used as the analytical peak for the sensor and biosensor from which the calibration curves were constructed. The peak was assigned to the oxidation

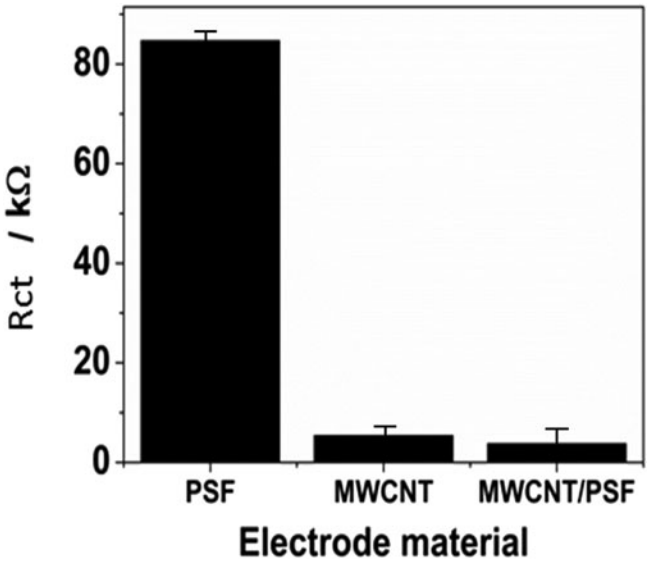

Figure 5. Response of the charge transfer resistance (Rct, kΩ) obtained from the equivalent circuit modeling of impedance measurements for polysulfone (PSF), multiwalled carbon nanotubes (MWCNT) and the combined (MWCNT/PSF) modified glassy carbon electrode measured at 0.7 V versus Ag/AgCl in 0.1 M PBS at pH 7.0.

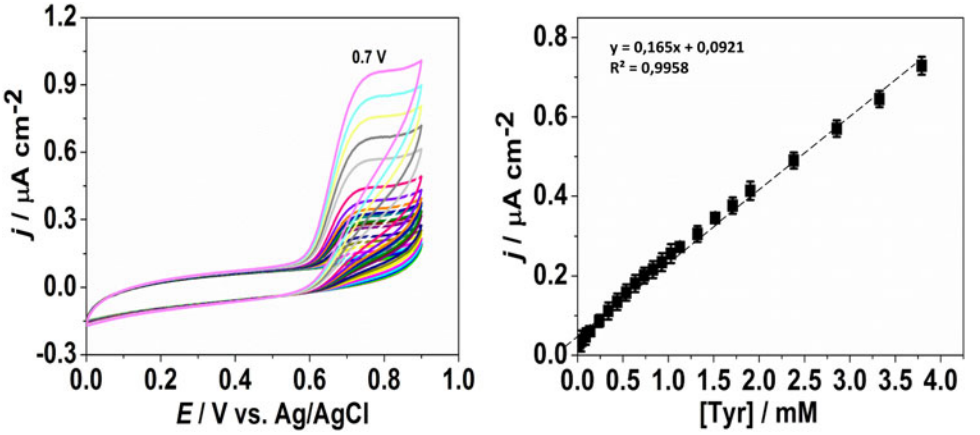

Figure 6. (a) Cyclic voltammograms for L-tyrosine oxidation at MWCNT/PSF/GCE versus Ag/AgCl at 50 mV s^{-1} across the concentration range from 1.96×10^{-6} to 3.94×10^{-4} M in PBS at pH 7 and (b) corresponding calibration curve for L-tyrosine ($n = 3$).

of tyrosine to L-Dopa (Fauziyah et al. 2012). The biosensor displayed a lower limit of detection and higher sensitivity, due to the presence of the enzyme (Table 2). The measurements were repeated three times ($n = 3$).

The performance of the biosensor was compared with other L-tyrosine sensors reported in the literature (Table 3). The limit of detection obtained in this work for L-tyrosine at the TyrOx/MWCNT/PSF/GCE biosensors was at least 2 orders of magnitude

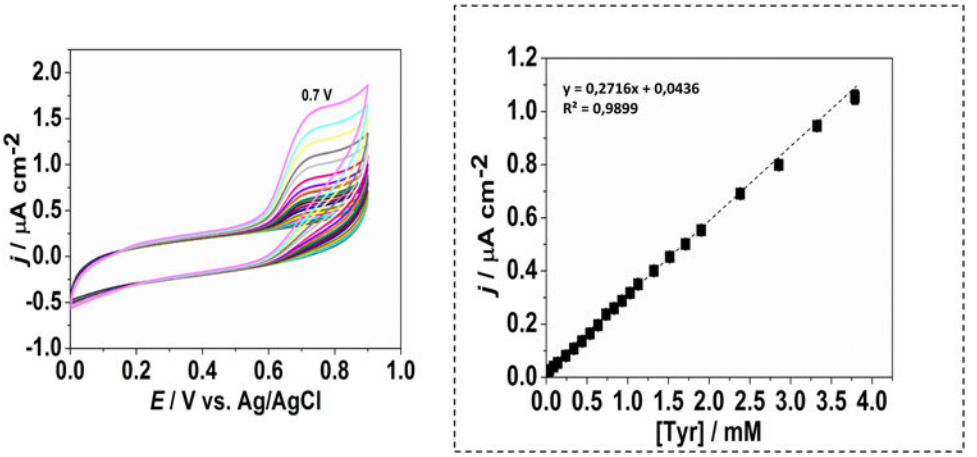

Figure 7. (a) Cyclic voltammograms for L-tyrosine oxidation at TyrOx/MWCNT/PSF/GCE versus Ag/AgCl at 50 mV s^{-1} across the concentration range from 1.96×10^{-6} to 3.94×10^{-4} M in PBS at pH 7 and (b) corresponding calibration curve for L-tyrosine ($n = 3$).

Table 2. Analytical performance of the L-tyrosine sensor and tyrosinase biosensor.

Electrode material	Limit of detection (M)	Sensitivity ± standard deviation ($n = 3$), (µA $µM^{-1}$)
MWCNT/PSF/GCE	2.5×10^{-9} (sensor)	19.0 ± 0.532
TyOx/MWCNT/PSF/GCE	3.06×10^{-10} (biosensor)	28.0 ± 0.182

Table 3. Comparison of sensor performance to similar biosensors reported in the literature.

Electrode Material	Sensitivity (µA $µM^{-1}$)	Limit of detection (nM)	Reference
hemin DNA biosensor	0.48	75	Wei et al. (2012)
Thionine aptasensor	2.62	130	Li et al. (2014)
Tyrosinase polymer biosensor	28	0.30	This work
Tyrosinase, carbon nanotubes biosensor	0.74	620	Apetrei and Apetrei (2013)
Tyrosinase polymer biosensor	4.81	1000	Hnida et al. (2015)

lower than obtained in most other literature reports, and the sensitivity of the biosensor was at least 2 orders of magnitude higher than the other reported values.

Conclusion

The effects of semiconducting PSF and MWCNT on the oxidation of L-tyrosine were evaluated by scanning electron microscopy, cyclic voltammetry and EIS.

The SEM imaging of the composite MWCNT/PSF confirmed characteristics of both PSF and MWCNT when compared to the images of the individual materials. The MWCNT/PSF/GCE composite shows the highest oxidative currents measured by CV and the lowest R_{ct} values, as derived from equivalent circuit modeling of the fixed potential impedance measurements. The MWCNT/PSF/GCE composite electrode was used in the design of an electrochemical sensor (MWCNT/PSF/GCE) and biosensor (TyrOx/MWCNT/PSF/GCE) for the analytical determination of L-tyrosine using cyclic

voltammetry. The biosensor displayed exceptional performance in terms of limits of detection and sensitivity towards L-tyrosine compared to recent literature reports for composite catalytic anodes.

Funding

This work was funded by the Marie Curie International Research, Commission of the European Communities project 318053 "SmartCancerSens" project.

References

Akyilmaz, E., E. Yorganci, and E. Asav. 2010. Do copper ions activate tyrosinase enzyme? A biosensor model for the solution. *Bioelectrochemistry* 78(2):155–160. doi:10.1016/j.bioelechem.2009.09.007.

Apetrei, I. M., and C. Apetrei. 2013. Biosensor based on tyrosinase immobilized on a single-walled carbon nanotube-modified glassy carbon electrode for detection of epinephrine. *International Journal of Nanomedicine* 8:4391–4398. doi:10.2147/IJN.S52760.

Bidsorkhi, H. C., H. Riazi, D. Emadzadeh, M. Ghanbari, T. Matsuura, W. J. Lau, and A. F. Ismail. 2016. Preparation and characterization of a novel highly hydrophilic and antifouling polysulfone/nanoporous TiO_2 nanocomposite membrane. *Nanotechnology* 27(41): 415706–415711. doi:10.1088/0957-4484/27/41/415706.

Carvalho, R. C., C. Gouveia-Caridade, and C. M. A. Brett. 2010. Glassy carbon electrodes modified by multiwalled carbon nanotubes and poly (neutral red): A comparative study of different brands and application to electrocatalytic ascorbate determination. *Analytical and Bioanalytical Chemistry* 398(4):1675–1685. doi:10.1007/s00216-010-3966-3.

Connell, M. J. O., P. Boul, L. M. Ericson, C. Hu, Y. Wang, E. Haroz, C. Kuper, J. Tour, K. D. Ausman, and R. E. Smalley. 2001. Reversible water-solubilization of single-walled carbon nanotubes by polymer wrapping. *Chemical Physics Letters* 342:265–271. doi:10.1016/S0009-2614(01)00490-0.

Dyachkova, T. P., A. V. Melezhyk, S. Y. Gorsky, I. V. Anosova, and A. G. Tkachev. 2013. Some aspects of functionalization and modification of carbon nanomaterials. *Nanosystems: Physics, Chemistry, Mathematics* 4(5):605–621.

Fauziyah, S., S. Gobikrishnan, N. Indrawan, S.-h. Park, J.-h. Park, K. Min, Y. Je Yoo, and D.-h. Park. 2012. A study on the electrochemical synthesis of L-DOPA using oxidoreductase enzymes: optimization of an electrochemical process. *Journal of Microbiology and Biotechnology* 22(10):1446–1451. doi:10.4014/jmb.1206.0604322:1446–51.

Hnida, K., G. Sulka, P. Knihnicki, J. Kozak, and A. Gilowska. 2015. Short communication: application of polypyrrole nanowires for the development of a tyrosinase biosensor. *Chemical Papers* 69(8):1130–1135. doi:10.1515/chempap-2015-0114.

Karim, N., and H. Jin. 2013. Amperometric phenol biosensor based on covalent immobilization of tyrosinase on Au nanoparticle modified screen printed carbon electrodes. *Talanta* 116: 991–996. doi:10.1016/j.talanta.2013.08.003.

Kaushik, V., H. Sharma, A. K. Shukla, V. D. Vankar, V. Kaushik, H. Sharma, A. K. Shukla, and V. D. Vankar. 2012. Modification in surface morphology and enhanced field emission properties of pristine carbon nanotubes by introducing nitrogen gas modification in surface morphology and enhanced field emission properties of pristine carbon nanotubes by introducing nitrogen gas. *AIP Conference Proceedings* 1451: 148. doi:10.1063/1.4732396.

Ke, G., W. Guan, C. Tang, W. Guan, D. Zeng, and F. Deng. 2007. Covalent functionalization of multiwalled carbon nanotubes with a low molecular weight chitosan. *Biomacromolecules* 8(2): 322–326. doi:10.1021/bm0604146.

Kim, K. S., K. H. Lee, K. Cho, and C. E. Park. 2002. Surface modification of polysulfone ultrafiltration membrane by oxygen plasma treatment. *Journal of Membrane Science* 199(1-2): 135–145. doi:10.1002/app.1994.070510120.

Koziol, K., B. O. Boskovic, and N. Yahya. 2010. Synthesis of carbon nanostructures by CVD method. *Advanced Structured Materials* 5:23–49. doi:10.1007/8611_2010_12.

Ly, S. Y., H. S. Yoo, and C. H. Lee. 2012. Voltammetric assay of antibiotics for modified carbon nanotube sensor. *Journal of Korean Oil Chemists' Society* 29(3):443–449.

Li, F., Y. Guo, X. Sun, and X. Wang. 2014. Aptasensor based on thionine, graphene – polyaniline composite film, and gold nanoparticles for kanamycin detection. *European Food Research and Technology* 239(2):227–236. doi:10.1007/s00217-014-2211-2.

Litescu, S. C., S. Eremia, and G. L. Radu. 2010. Biosensors for the determination of phenolic metabolites. In Bio-Farms for Nutraceuticals: Functional Food and Safety Control by Biosensors. Chapter 17:234–240. Boston: Springer.

Lupu, S., C. Lete, P. Balaure, D. Caval, C. Mihailciuc, B. Lakard, J.-Y. Hihn, and F. Campo. 2013. Development of amperometric biosensors based on nanostructured tyrosinase-conducting polymer composite electrodes. *Sensors* 13(5):6759–6774. doi:10.3390/s130506759.

Ma, Q., S. Ai, H. Yin, Q. Chen, and T. Tang. 2010. Electrochimica acta towards the conception of an amperometric sensor of L-tyrosine based on hemin/PAMAM/MWCNT modified glassy carbon electrode. *Electrochimica Acta* 55(22):6687–6694. doi:10.1016/j.electacta.2010.06.003.

Muya, F. N., L. Phelane, P. G. L. Baker, and E. I. Iwuoha. 2014. Synthesis and characterization of polysulfone hydrogels. *Journal of Surface Engineered Materials and Advanced Technology* 04(04):227–236. doi:10.4236/jsemat.2014.44025.

Park, J. Y., Acar, M. H. A. Akthakul, W. Kuhlman, and A. M. Mayes. 2006. Polysulfone- graft -poly(ethylene glycol) graft copolymers for surface modification of polysulfone membranes. *Biomaterials* 27(6):856–865. doi:10.1016/j.biomaterials.2005.07.010.

Peça, R. C., M. Bertotti, and M. A. Brett. 2011. Methylene blue/multiwall carbon nanotube modified electrode for the amperometric determination of hydrogen peroxide. *Electroanalysis* 23(10):2290–2296. doi:10.1002/elan.201100324.

Phelane, L., F. N. Muya, H. L. Richards, P. G. L. Baker, and E. I. Iwuoha. 2014. Polysulfone nanocomposite membranes with improved hydrophilicity. *Electrochimica Acta* 128:326–335. doi:10.1016/j.electacta.2013.11.156.

Qiu, S., Li. Wu, X. Pan, L. Zhang, H. Chen, and C. Gao. 2009. Preparation and properties of functionalized carbon nanotube/PSF blend ultrafiltration membranes. *Journal of Membrane Science* 342(1-2):165–172. doi:10.1016/j.memsci.2009.06.041.

Revin, S. B., and S. A. John. 2013. Electrochemical marker for metastatic malignant melanoma based on the determination of L -Dopa/L -Tyrosine ratio. *Sensors and Actuators B: Chemical* 188:1026–1032. doi:10.1016/j.snb.2013.08.019.

Samuel, S., M. Pumera, and F. Esteve. 2007. Carbon nanotube/polysulfone screen-printed electrochemical immunosensor. *Biosensors and Bioelectronics* 23:332–340. doi:10.1016/j.bios.2007.04.021.

Sanz, V. C., M. Luz Mena, A. Gonz, and J. M. Pingarr. 2005. Development of a tyrosinase biosensor based on gold nanoparticles-modified glassy carbon electrodes application to the measurement of a bioelectrochemical polyphenols index in wines. *Analytica Chimica Acta* 528:1–8. doi:10.1016/j.aca.2004.10.007.

Singjai, P., S. Changsarn, and S. Thongtem. 2007. Electrical resistivity of bulk multi-walled carbon nanotubes synthesized by an infusion chemical vapor deposition method. *Materials Science and Engineering: A* 443(1-2):42–46. doi:10.1016/j.msea.2006.06.042.

Wang, S., Y. Tan, D. Zhao, and G. Liu. 2008. Amperometric tyrosinase biosensor based on Fe_3O_4 nanoparticles – chitosan nanocomposite. *Biosensors and Bioelectronics* 23(12):1781–1787. doi: 10.1016/j.bios.2008.02.014.

Wang, Y., X. Zhang, Y. Chen, H. Xu, Y. Tan, and S. Wang. 2010. Detection of dopamine based on tyrosinase- Fe_3O_4 nanoparticles-chitosan nanocomposite biosensor. *American Journal of Biomedical Sciences* 2(3):209–216. doi:10.5099/aj100300209.

Wei, J., J. Qiu, L. Li, L. Ren, X. Zhang, J. Chaudhuri, and S. Wang. 2012. A reduced graphene oxide based electrochemical biosensor for tyrosine detection. *Nanotechnology* 23(33):335707. doi:10.1088/0957-4484/23/33/335707.

Xu, Q., and S. Wang. 2005. Electrocatalytic oxidation and direct determination of l-tyrosine by square wave voltammetry at multi-wall carbon nanotubes modified glassy carbon electrodes. *Microchimica Acta* 52:47–52. doi:10.1007/s00604-005-0408-6.